



Contents lists available at ScienceDirect

Journal of Pharmaceutical Analysis

journal homepage: www.elsevier.com/locate/jpa

Original Article

Irbesartan desmotropes: Solid-state characterization, thermodynamic study and dissolution properties



Andrea Mariela Araya-Sibaja ^{a, b, c}, Carlos Eduardo Maduro de Campos ^d,
Cinira Fandaruff ^e, José Roberto Vega-Baudrit ^{a, f}, Teodolito Guillén-Girón ^b,
Mirtha Navarro-Hoyos ^c, Silvia Lucía Cuffini ^{g, *}

^a Laboratório Nacional de Nanotecnologia LANOTEC-CeNAT-CONARE, 1174-1200, Pavas, San José, Costa Rica

^b Escuela de Ciencia e Ingeniería de los Materiales, Tecnológico de Costa Rica, Cartago, 159-7050, Costa Rica

^c Escuela de Química, Universidad de Costa Rica, San Pedro de Montes de Oca, 2060, San José, Costa Rica

^d Programa de Pós-Graduação em Física, Universidade Federal de Santa Catarina, Florianópolis, Brazil

^e Independent Researcher, 06472-005, Barueri, São Paulo, Brazil

^f Laboratorio de Investigación y Tecnología de Polímeros POLIUNA, Escuela de Química, Universidad Nacional de Costa Rica, Heredia, 86-3000, Costa Rica

^g Instituto de Ciência e Técnica, Universidade Federal de São Paulo, São José dos Campos, São Paulo, Brazil

ARTICLE INFO

Article history:

Received 4 February 2019

Received in revised form

8 July 2019

Accepted 9 July 2019

Available online 10 July 2019

Keywords:

Irbesartan

Solid-state characterization

Intrinsic dissolution rate

Tautomerism

Desmotropic forms

ABSTRACT

Irbesartan (IBS) is a tetrazole derivative and antihypertensive drug that has two interconvertible structures, 1H- and 2H-tautomers. The difference between them lies in the protonation of the tetrazole ring. In the solid-state, both tautomers can be isolated as crystal forms A (1H-tautomer) and B (2H-tautomer). Studies have reported that IBS is a polymorphic system and its forms A and B are related monotropically. These reports indicate form B as the most stable and less soluble form. Therefore, the goal of this contribution is to demonstrate through a complete solid-state characterization, thermodynamic study and dissolution properties that the IBS forms are desmotropes that are not related monotropically. However, the intention is also to call attention to the importance of conducting strict chemical and in solid-state quality controls on the IBS raw materials. Hence, powder X-ray diffraction (PXRD) and Raman spectroscopy (RS) at ambient and non-ambient conditions, differential scanning calorimetry (DSC), hot stage microscopy (HSM), Fourier transform infrared (FT-IR) and scanning electron microscopy (SEM) techniques were applied. Furthermore, intrinsic dissolution rate (IDR) and structural stability studies at 98% relative humidity (RH), 25 °C and 40 °C were conducted as well. The results show that in fact, form A is approximately four-fold more soluble than form B. In addition, both IBS forms are stable at ambient conditions. Nevertheless, structural and/or chemical instability was observed in form B at 40 °C and 98% RH. IBS has been confirmed as a desmotropic system rather than a polymorphic one. Consequently, forms A and B are not related monotropically.

© 2019 Xi'an Jiaotong University. Production and hosting by Elsevier B.V. This is an open access article under the CC BY-NC-ND license (<http://creativecommons.org/licenses/by-nc-nd/4.0/>).

1. Introduction

Molecular compounds that present tautomerism can be characterized as polymorphs or desmotropes in the solid-state [1–3]. Polymorphic forms are different crystalline phases obtained from the identical molecular compound in terms of atom connectivity

[4–6]. Although some authors extend this definition to geometric isomers, enantiomers and tautomers [1,6,7], the formation of tautomers implies the breaking and forming of bonds [8]. In this sense, when the different tautomers crystallize independently, this phenomenon is known as desmotropy, and the crystals formed are named desmotropes [1–3]. In some compounds, polymorphic and desmotropic forms [9] and two tautomers in the same crystal lattice [10] have been observed. It is well known that the polymorphs exhibit different pharmaceutical properties such as solubility and stability, which are associated with bioavailability, manufacturing and storage issues [3,11–13]. Differences are also exhibited in the case of desmotropes since they present not only different

Peer review under responsibility of Xi'an Jiaotong University.

* Corresponding author at: Instituto de Ciência e Tecnologia, Universidade Federal de São Paulo. Rodovia Presidente Dutra, do km 144,000 ao km 144,999 (lado direito), Jardim Diamante, São José dos Campos, SP - CEP: 12.223-201, Brazil.

E-mail address: scuffini@unifesp.br (S.L. Cuffini).

<https://doi.org/10.1016/j.jpha.2019.07.001>

2095-1779/© 2019 Xi'an Jiaotong University. Production and hosting by Elsevier B.V. This is an open access article under the CC BY-NC-ND license (<http://creativecommons.org/licenses/by-nc-nd/4.0/>).

crystalline structures but also different chemical entities [1,14]. There is general agreement, therefore, about the importance of the study of these phenomena [5,6,15]. Hence, to establish thermodynamic stability among crystal forms is a critical concern. Indeed, the study of these phenomena constitutes an essential part of pharmaceutical research and development [12,16].

Irbesartan (IBS), 2-butyl-3-[[4-[2-(2-{H}-tetrazol-5-yl)phenyl]phenyl]methyl]-1,3-diazaspiro[4.4]non-1-en-4-one [17] (Fig. 1) is an antihypertensive drug. It acts by inhibiting the renin-angiotensin system by selectively blocking the AT1 subtype of receptors [18]. IBS is a type of N-substituted heterocycle derivative that exhibits tautomerism [19]. In solution, 1H and 2H-tautomers exhibit similar energy and the equilibrium towards one to the other species is quite sensitive to the chemical environment [20]. In the annular tautomerism of azoles, the differences in energy among species should be quite low to have a reasonable probability to isolate two desmotropes [8]. In terms of energy, it is important to emphasize that the activation barrier between two species in solution cannot be used to differentiate between isomers, tautomers and polymorphs [8]. An evaluation in solution will give discrepancies for those related to conformational and configurational terms. Therefore, the evaluation needs to be done in the solid state [2,8,21].

Several IBS crystal forms reported up to date are summarized in Table 1, being of particular interest the desmotropic system occurring when tautomers 1H and 2H crystallize into forms A and B, respectively [22]. The difference between them involves an intramolecular proton transfer in the tetrazole ring, which, unassisted, results in a highly energetically demanding process [20,23–25]. Indeed, a solid-state proton transfer is not expected and has not been reported experimentally [20]. The literature describes IBS forms A and B as polymorphs related monotropically [26,27] with form B as the most thermodynamically stable, and form A as presenting significantly higher aqueous solubility than form B [11]. Indeed, pharmaceutical dosage forms of IBS are formulated using the form A [20]. However, considering the following aspects: i) there were previous recalls of IBS/hydrochlorothiazide composed tablets (Avalide®) due to the presence of the form B in the formulation that compromised the bioavailability of the product [28], ii) the recent withdrawing of IBS tablets from the market due to the presence of trace amounts of N-nitrosodiethylamine [29], and iii) regardless of whether the solid forms are desmotropes or polymorphs, they present differences in physicochemical properties, including chemical and physical stabilities [13]. Therefore, a concern about stricter quality control of IBS raw materials has arisen and both chemicals' solid-state analyses are required.

Therefore, a deep solid-state characterization, thermodynamic study and investigation into the dissolution properties of IBS solid

forms have been conducted. Given the relevance of this information for the pharmaceutical industry, structural stability at different ambient conditions was evaluated for both IBS solid forms.

2. Experimental

2.1. Chemicals

IBS raw material was kindly donated by CALOX of Costa Rica in its micronized form A. Form B was obtained by recrystallization of raw material in acetonitrile. IBS pharmaceutical secondary standard (traceable to USP and PhEur) Fluka brand was purchased from Sigma-Aldrich (Laramie, WY, USA). Acetonitrile was of HPLC/UV grade, and water was obtained by purification using a Millipore system filtered through a Millipore membrane 0.22 μm Millipak™ 40. All solvents were of HPLC/UV grade.

2.2. Characterization techniques

2.2.1. Powder X-ray diffraction (PXRD)

PXRD patterns at ambient conditions were collected from a PANalytical Empyrean diffractometer equipped with a Cu K α source ($\lambda = 1.5418\text{\AA}$) operated at 45 kV and 40 mA, step size 0.016° , step time 20 s, angular scanning speed $2^\circ/\text{min}$ and 2θ angular range between 4° and 50° using a silicon strip detector (PIXcel 1D). PXRD patterns at variable temperature were collected from a PANalytical X'PERT Multipurpose diffractometer equipped with a Cu K α source ($\lambda = 1.5418\text{\AA}$) operated at 45 kV and 40 mA, step size 0.016° , step time 20 s, angular scanning speed $2^\circ/\text{min}$ and 2θ angular range between 5° and 50° using a linear solid-state detector (Xcelerator). The samples were heated using an Anton Paar HTK16 camera from 25 to 134°C and cooled to 25°C at $10^\circ\text{C}/\text{min}$ rates, except during PXRD patterns acquisition (isotherms). The calculated PXRD pattern was carried out with a line width different from the experimental one.

2.2.2. Raman spectroscopy (RS) at ambient and variable temperature

Raman spectra were collected in backscattering geometry using a PeakSeeker 785 (RAM – PRO – 785) Raman system with a diode laser of 785 nm and 300 mW at the source. The collected Raman radiation was dispersed with a grating and focused on a Peltier-cooled charge-coupled device (CCD) detector allowing us to obtain a spectral resolution of 6 cm^{-1} . The LASER was focused on the sample by a $20\times$ objective lens of a microscope giving a spot of approximately $2\text{ }\mu\text{m}$ diameter. All spectra were recorded in the spectral window of $200\text{--}1800\text{ cm}^{-1}$ with the same acquisition time (30 s). The powders were analysed on glass slides at room temperature.

2.2.3. Fourier transform infrared (FT-IR)

FT-IR spectra of the sample were recorded on a Thermo Scientific Nicolet 6700 FT-IR equipment fitted with a diamond Attenuated Total Reflectance (ATR) accessory. The data were collected from 4000 to 600 cm^{-1} using 32 cm^{-1} . The samples were placed into the ATR cell without further preparation.

2.2.4. Differential scanning calorimetry (DSC)

DSC curves of the crystals produced were obtained in a DSC-Q200 (TA Instrument, New Castle, DE, USA) equipped with a TA Refrigerated Cooling System 90 using aluminium crucibles with approximately 2 mg of the sample under a dynamic nitrogen atmosphere ($50\text{ mL}/\text{min}$) and a heating rate of $10^\circ\text{C}/\text{min}$ in the temperature range from 40 to 200°C . The DSC cell was calibrated with a standard reference of indium.

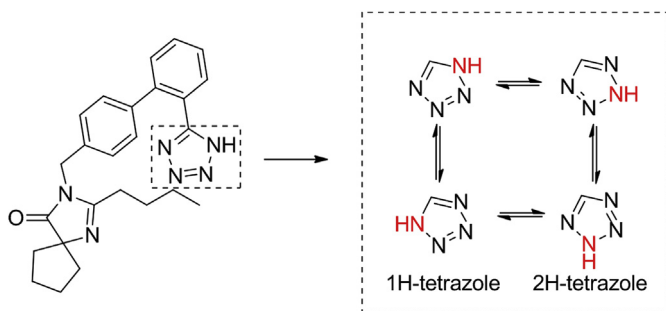


Fig. 1. Chemical structure of irbesartan and tautomerism in the tetrazole system (adapted from Ref. [22]).

Table 1
Crystal forms of IBS already reported in the literature.

Crystal form	Description
Form A	Crystal structure not reported in CSD
1	Trigonal ($R\bar{3}$) according to Refs. [30,31]. No cell parameters have been reported.
2	Monoclinic ($P2_1/c$) according to Ref. [32]. No cell parameters have been reported
3	Hexagonal system according to Ref. [27]. No more details have been given
4	Trigonal ($R\bar{3}$) according to Ref. [11] Crystal data: a: 37.269 Å α : 90.0° b: 37.269 Å β : 90.0° c: 9.793 Å γ : 120.0° V: 11779.91 Å ³ Z: 18
5	Monoclinic ($P2$) according to ICDD PDF-4 Organics 2018 [33]. Crystal data: a: 10.969 Å α : 90.00° b: 18.901 Å β : 98.27° c: 9.508 Å γ : 90.00° V: 1950.76 Å ³ Z: 4.00
Form B	CCSD ref code: NOZWII Triclinic ($P\bar{1}$) [18] Crystal data: a: 11.969 Å α : 90.75° b: 12.181 Å β : 105.24° c: 9.366 Å γ : 112.92° V: 1122.9 Å ³ Z: 2
Hydrochloride 1.69-hydrate	CCSD ref code: LIBZAY Monoclinic ($P2_1/a$) [34] Crystal data: a: 8.5557 Å α : 90.00° b: 25.0130 Å β : 104.415° c: 12.2675 Å γ : 90.00° V: 2542.64 Å ³ Z: 4
Bromide sesquihydrate	CCSD ref code: NIQVIT Monoclinic ($P2_1/c$) [35] Crystal data: a: 12.482 Å α : 90.00° b: 25.285 Å β : 105.78° c: 8.6938 Å γ : 90.00° V: 2640.4 Å ³ Z: 2
IBS: Hippuric acid cocrystal	Crystal structure not reported [36]

2.2.5. Hot-stage microscopy (HSM)

Thermal events were observed on an Olympus BX53 microscope equipped with a THMS600PS Linkam heating/cooling plate and a QICAM Fast 1394 camera. The samples were placed on a microscope slide, covered with a coverslip, and heated at a rate of 5 °C/min.

2.2.6. Scanning electron microscopy (SEM)

Micrographs were obtained from a JEOL JSM-6390 LV scanning electron microscope operated in the range of 5–30 kV. The samples were mounted on a metal stub using double-sided adhesive tape and coated under vacuum with gold in an argon atmosphere.

2.2.7. Intrinsic dissolution rate (IDR) test

The rotating disk method specified in USP30-NF25 1087 Intrinsic Dissolution was used. Approximately 100 mg of each IBS solid form was compacted into a 0.5 cm² surface using an ASTA hydraulic press with a manometer to 400 kg. The effect of the pressure in the solid state transition was monitored by PXRD. Samples were analysed in a VARIAN VK 7000 dissolution test system. The selected dissolution medium was 300 mL of sodium lauryl sulphate (SLS) 0.25% (w/v) previously heated at 37 °C \pm 0.5 °C. Analyses were carried out at a rotation speed of 75 rpm. Then, 5 mL of the samples were withdrawn at 5, 15, 30, 60, 90, 120, 180 and 240 min. To maintain a constant total volume, a 5 mL aliquot of preheated fresh medium was replaced into the vessels after each sample was removed. The sample aliquots were filtered and then analysed using a Varian Cary 50 Bio spectrophotometer at 240 nm.

The sink conditions were maintained during the whole dissolution experiment.

2.3. Structural stability under solid-state stress conditions

IBS crystal forms A and B were placed individually on glass slides with a single depression concavity. The samples were stored at 25 °C and 40 °C, both at 98% relative humidity (RH), for 4 months. The 98% RH was achieved with a K₂SO₄ saturated solution. Samples were analysed by PXRD at 0, 3, 15, 30, 60, 90 and 120 days.

3. Results and discussion

3.1. Characterization of IBS desmotropes

3.1.1. PXRD analyses

In the Cambridge Structural Database (CSD), only the crystallographic data NOZWII for IBS form B is available. Although there are several reports of IBS form A indicated as trigonal [11,30,31] and monoclinic [32,33] with quite different cell parameters (Table 1 [18,27,34–36]), its crystal structure has not been deposited in the CSD. Therefore, the experimental powder pattern of the raw material that agrees with the literature [18] was used to identify form A, whereas the calculated powder pattern from NOZWII was employed in the identification of form B. These patterns are presented in Fig. 2, showing several superimposed reflections. However, each solid form presents characteristic reflections that allow

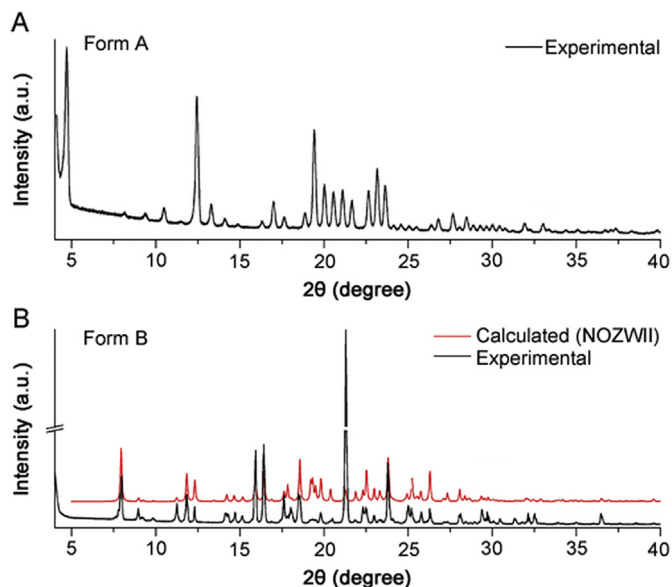


Fig. 2. PXRD pattern of IBS desmotropic forms: (A) experimental form A and (B) experimental and calculated form B (NOZWII crystallographic data).

the differentiation of both crystal forms. The selected reflections used in this contribution were 4.70, 13.24, 20.01, and 23.10 to identify form A, while 7.91, 11.80, 15.91, 18.55 and 19.87 were chosen to identify form B.

3.1.2. Fourier transform infrared (FT-IR) and Raman spectroscopy (RS)

Considering that IBS desmotropes are chemically different by the protonation of the tetrazole ring, different patterns in their vibrational modes are expected. However, the bands associated with imidazole and tetrazole groups are difficult to interpret and assign [37]. Nonetheless, the comparative FT-IR spectra of IBS forms A and B showed differences in three zones of the spectra. The first approximately 3000 cm^{-1} corresponded to C-H stretching; two bands shifted from 1730 and 1615 to 1725 and 1620 cm^{-1} from form A to solid form B, as can be observed at the bottom of Fig. 3A. This zone is related to C=O stretching and N-H bending, respectively. The third zone is located from 1200 to 600 cm^{-1} , including the absence of the band at 778 cm^{-1} in form B, which is associated with the NH out-of-plane bending mode of the CNH moiety only present in form A [37]. Another characteristic band that can be used to distinguish between forms A and B appears at 1006 cm^{-1} and is present only in form B and is related to NNN bending. Through the Raman spectra in Fig. 3B, it is possible to observe the differences in some regions when comparing both IBS solid forms, mainly between 250 and 500 cm^{-1} and 950– 1150 cm^{-1} . The detailed figures at the bottom of Fig. 3B clearly show the mentioned differences. Approximately 325– 375 cm^{-1} the Raman spectra show three new bands for crystal form B as well as two new bands approximately 400 cm^{-1} . A strong band observed only in form B at 995 cm^{-1} is related to NNN bending. An intense band at 1245 cm^{-1} in form B spectra is due to NNH bending. These results are in agreement with those reported in the literature [37,38]. Moreover, it can be noticed that the peak intensity in the Raman spectra of form B is clearly higher for the full spectral range examined.

3.1.3. SEM

Micrographs in Fig. 4 show the crystal habit of IBS solid forms

with different morphologies; while form A crystallizes in a thin needle-like shape, form B presents a large prism shape. These morphologies are in agreement with those reported in the literature for this desmotropic antihypertensive drug [22,30].

3.1.4. DSC, HSM, variable temperature PXRD and RS

DSC curves in Fig. 5 show an independent endothermic event for each IBS desmotropic form at $182.35\text{ }^{\circ}\text{C}$ in form A and at $185.66\text{ }^{\circ}\text{C}$ in form B's DSC curve. There is no evidence of any other exothermic or endothermic event in any of the solid forms' DSC curves that suggests a solid-solid phase transition or recrystallization during heating. The melting temperature of IBS form A is reported in the DRUGBANK website [39] as 180 and $181\text{ }^{\circ}\text{C}$. These values agree with the DSC data presented in Fig. 5. However, there are no other data reported for form A and no data are available for crystal form B. The HSM images are in concordance with the DSC curves: the DSC curves do not show a different phenomenon other than melting during the evaluation of each IBS solid form.

Variable temperature PXRD and HSM also confirmed there is no solid-state transition induced by temperature in the IBS crystal forms. Fig. 6 presents the PXRD patterns of both IBS solid forms with no new reflections arising during the heating program until a melting event at $190\text{ }^{\circ}\text{C}$. The same was observed in Fig. 7 for RS measures. There are no changes in the RS spectra during the temperature increases.

3.1.5. IDR determination

The solubilities of form A [40] and form B [19] have been reported in different organic solvents and ethanol-water mixtures, respectively. However, the IDR value has been considered to be better and more useful than solubility to correlate the in vivo drug dissolution dynamics [41]. According to Šehić et al., [42] values lower than 1 mg/min/cm^2 indicate dissolution rate-limiting absorption. Under sink conditions, the IDR for two crystal forms of a drug must be proportional to the respective solubilities [43]. Solubility and IDR are available for the amorphous form and form A [26]; however, they are not available for form B or for comparisons among the desmotropic forms. Fig. 8 shows a linear behaviour in the intrinsic dissolution profile of both IBS forms A and B. The IDR of form A was $0.017 \pm 0.004\text{ mg/min/cm}^2$ and $0.004 \pm 0.001\text{ mg/min/cm}^2$ for form B, indicating that form A is approximately four-fold more soluble than form B.

3.2. Relative thermodynamic stabilities between IBS desmotropes

To confirm that forms A and B are not monotonically related as previously described in the literature [26,27], the thermodynamic rules that should be considered in the evaluation of the relative thermodynamic stability between polymorphs were applied in this work. The rules used herein were summarized by Lee et al. [44] in a guide for pharmaceutical crystal form screening and selection. However, considerations to be aware of in the case of desmotropes have not been included [44]. The rules comprise determination of heat and entropy of fusion through DSC analyses. HSM, variable temperature PXRD and RS analyses support the results obtained by the DSC data. IDR tests give the data for the solubility rule and structural stability under solid-state stress conditions to complement this study.

The DSC curves and HSM analysis are presented in Fig. 5, showing no endothermic event associated with a phase transition. In addition, variable temperature PXRD and variable temperature RS confirm the absence of solid phase transitions induced by the temperature increase (Figs. 6 and 7). To establish no significant changes in the melting values of IBS desmotropes, DSC curves were run in triplicate. From these DSC curves the average melting

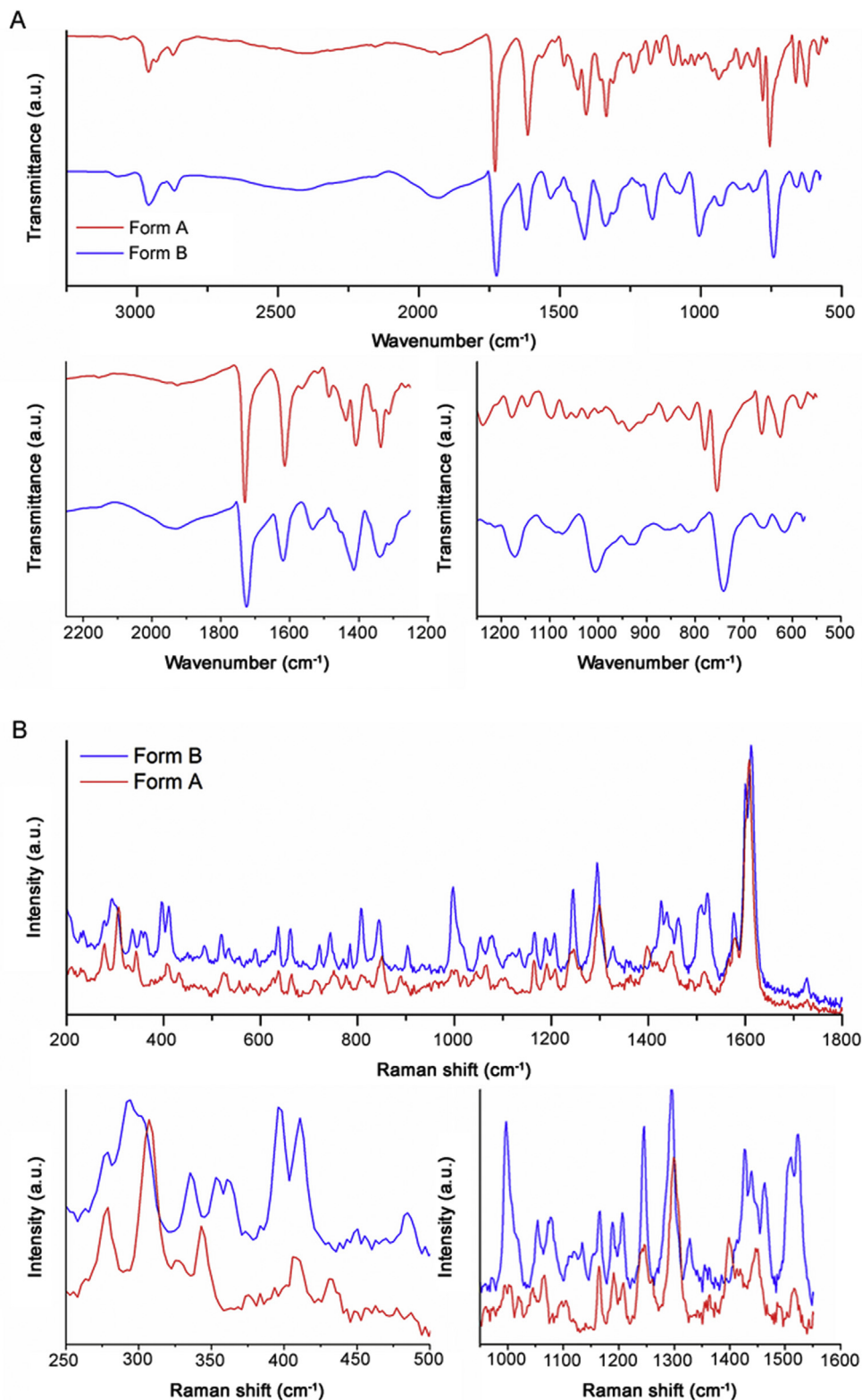


Fig. 3. IBS desmotropic forms A and B: (A) FT-IR spectra and (B) Raman spectra.

temperature of form A was 184.2 ± 0.2 °C with an associated enthalpy of fusion of 89 ± 2 J/g. In the case of crystal form B, a melting temperature of 186.7 ± 0.1 °C and a value of 115 ± 3 J/g for the enthalpy were obtained. Calculating the entropy of fusion using the data obtained from the DSC curves, form A presents an entropy

of fusion of 0.48 J/g/K and form B of 0.62 J/g/K. In the solubility rule, IDR profiles were determined, which according to Lee et al. [44] should be performed at the transition temperature observed in the DSC and/or HSM analyses. In this case, no transition was observed between these two crystal forms. Hence, IDR was determined at

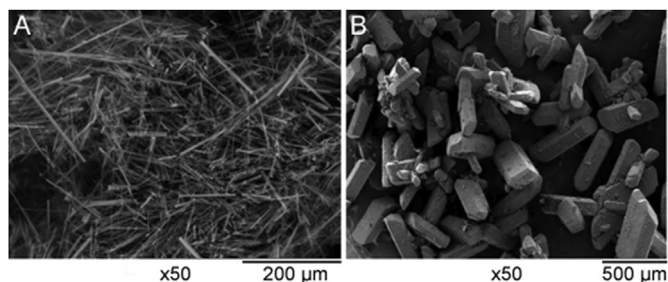


Fig. 4. SEM micrographs of both IBS desmotropes: (A) form A and (B) form B.

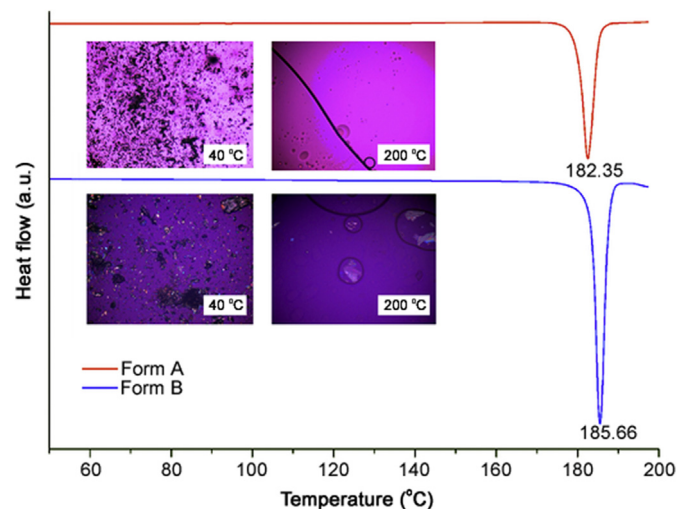


Fig. 5. DSC curves and inserted HSM images of IBS desmotropic forms A and B.

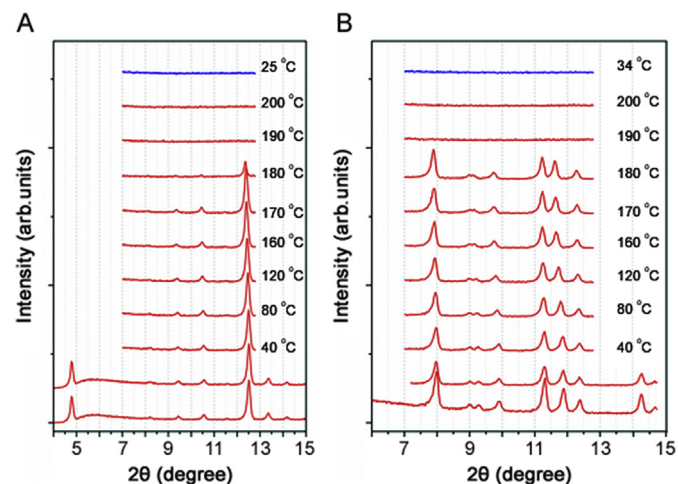


Fig. 6. Non-ambient temperature PXRD patterns of IBS solid forms: (A) form A and (B) form B.

37.5 °C in sodium lauryl sulphate 0.25%. IDR profiles are presented in Fig. 8, in which form A has the highest intrinsic dissolution rate, and, therefore, the highest solubility.

Therefore, the following results are obtained: 1) there is no temperature transition observed for IBS crystal forms, confirmed by DSC, HSM, variable temperature PXRD and RS. 2) Form A has the lower melting point and the lower heat of fusion. 3) Form A exhibits the lowest melting point and the lowest entropy of fusion. It is also

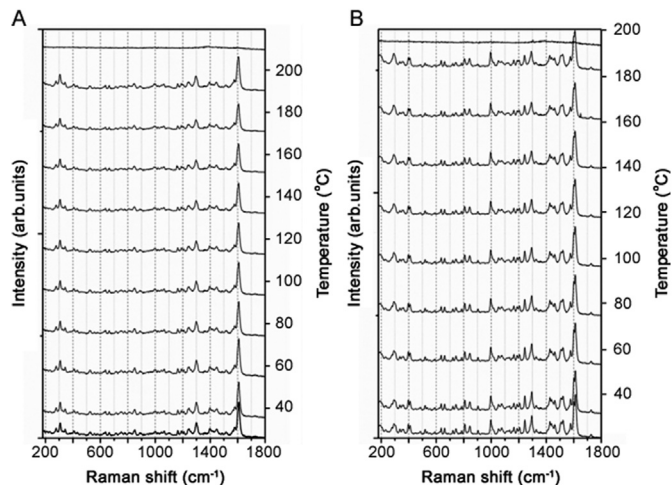


Fig. 7. Non-ambient temperature Raman spectra of IBS solid forms: (A) form A and (B) form B.

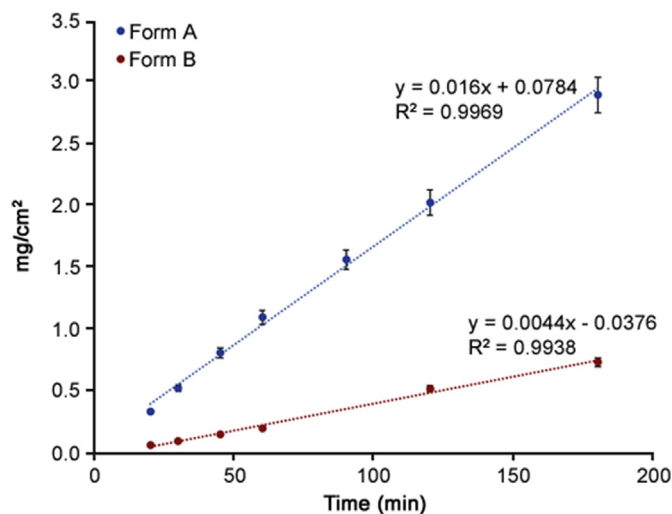


Fig. 8. IDR profile of both IBS desmotropes.

important to highlight that both solid forms A and B exhibited a solid state and structural stability at room temperature. Furthermore, the results from ongoing research in our group have demonstrated the influence of solvent polarity on crystallization of forms A and B. Therefore, form A was obtained from a less polar solvent such as ethanol, and form B was crystallized from the highly polar solvent water. Moreover, in a less polar solvent form B transformed into form A and in a highly polar solvent form A transformed into form B [45]. These results indicate that both IBS desmotropic forms A and B are thermodynamically stable, and they are not true polymorphs nor are they monotropically related.

In other ambient conditions, form B showed modifications after one month of storage under 98% RH and 40 °C. In Fig. 9 a diffractogram can be observed, showing the reflections at 7.87° and 15.85° splitting into 2 reflections. From the third month, a new reflection arising at 7.64° was observed. None of these reflections were related to the powder pattern of form A. This suggests a solid-state transition to an unknown crystalline structure or chemical degradation.

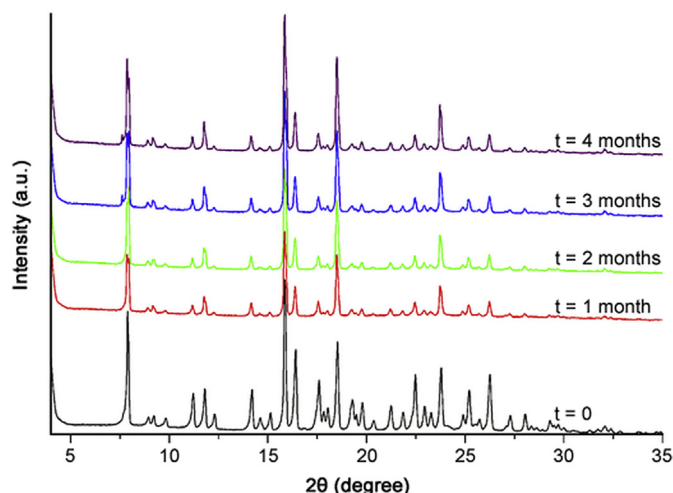


Fig. 9. PXRD patterns of IBS form B at different times of storage at 98% RH and 40 °C.

4. Conclusions

IBS crystalline forms A and B were characterized by PXRD, DSC, HSM, SEM, FT-IR, RS and IDR profiles. As expected from their different chemical nature and structures, forms A and B exhibited variations in their physicochemical properties. Form A presented a higher solubility and intrinsic dissolution rate than form B, and form B was unstable at high humidity and higher temperatures. However, forms A and B were both stable at ambient conditions. This solid-state characterization of IBS could be very useful for current and/or new applications in the pharmaceutical industry.

Acknowledgments

This research was made possible by the financial support of FEES-CONARE (Ref 115B5662), the University of Costa Rica (UCR), the Costa Rica Institute of Technology (TEC) and the National Laboratory of Nanotechnology (LANOTEC). The authors thank the PINN program (PI-0132-15) of the Ministry of Science Technology and Telecommunications (MICITT) of Costa Rica and the Postgraduate Office of the TEC by the doctoral scholarships granted to Andrea M. Araya-Sibaja. The authors are grateful for the collaboration provided by the Universidade Federal de Santa Catarina, Brazil by its laboratories: Laboratório de Difrração de Raios-X (LDRX) for the variable temperature PXRD and variable temperature Raman analyses, and Laboratório de Controle de Qualidade for the IDR determinations.

Conflicts of interest

The authors declare that there are no conflicts of interest.

Appendix A. Supplementary data

Supplementary data to this article can be found online at <https://doi.org/10.1016/j.jpha.2019.07.001>.

References

- [1] A.R. Katritzky, C.A. Ramsden, J.A. Joule, et al., Structure of five-membered rings with two or more heteroatoms, in: *Handb. Heterocycl. Chem.*, 2010, pp. 139–209.
- [2] J. Elguero, Polymorphism and desmotropy in heterocyclic crystal structures, *Cryst. Growth Des.* 11 (2011) 4731–4738.
- [3] V.B. Kurteva, B.L. Shivachev, R.P. Nikolova, et al., Conformational behaviour of 3-methyl-4-(4-methylbenzoyl)-1-phenyl-pyrazol-5-one: a sudden story of three desmotropes, *RSC Adv.* 5 (2015) 73859–73867.
- [4] H.G. Brittain, Polymorphism and solvatomorphism 2010, *J. Pharm. Sci.* 101 (2012) 464–484.
- [5] H. Brittain, Polymorphism in pharmaceutical solids, *J. Control. Release* 71 (2001) 354–355.
- [6] J. Bernstein, *Polymorphism in Molecular Crystals*, Oxford University Press, 2007.
- [7] D. Braga, F. Grepioni, L. Maini, The growing world of crystal forms, *Chem. Commun.* 46 (2010) 6232–6242.
- [8] M.A. García, C. López, R.M. Claramunt, et al., Polymorphism vs. desmotropy: the cases of 3-phenyl- and 5-phenyl-1H-pyrazoles and 3-phenyl-1H-indazole, *Helv. Chim. Acta* 85 (2002) 2763–2776.
- [9] A.J. Cruz-Cabeza, C.R. Groom, Identification, classification and relative stability of tautomers in the Cambridge structural database, *CrystEngComm* 13 (2011) 93–98.
- [10] C. Wales, L.H. Thomas, C.C. Wilson, Tautomerisation and polymorphism in molecular complexes of piroxicam with mono-substituted benzoic acids, *CrystEngComm* 14 (2012) 7264–7274.
- [11] S.P. Delaney, D. Pan, M. Galella, et al., Understanding the origins of conformational disorder in the crystalline polymorphs of irbesartan, *Cryst. Growth Des.* 12 (2012) 5017–5024.
- [12] C. Gu, D.J.W. Grant, Estimating the relative stability of polymorphs and hydrates from heats of solution and solubility data, *J. Pharm. Sci.* 90 (2001) 1277–1287.
- [13] H. Bourichi, Y. Brik, P. Hubert, et al., Solid-state characterization and impurities determination of fluconazole generic products marketed in Morocco, *J. Pharm. Anal.* 2 (2012) 412–421.
- [14] J. Elguero, Tautomerism: A Historical Perspective, in: *Tautomerism*, Wiley-VCH Verlag GmbH & Co. KGaA, Weinheim, Germany, 2016, pp. 1–10.
- [15] O.M.M. Santos, M.E.D. Reis, J.T. Jacon, et al., Polymorphism: an evaluation of the potential risk to the quality of drug products from the Farmácia Popular Rede Própria, *Brazilian J. Pharm. Sci.* 50 (2014) 1–24.
- [16] A. Burger, R. Ramberger, On the polymorphism of pharmaceuticals and other molecular crystals. II, *Mikrochim. Acta* 72 (1979) 273–316.
- [17] PubChem, Irbesartan. <https://pubchem.ncbi.nlm.nih.gov/compound/irbesartan#section=Names-and-Identifiers>, 2018. (Accessed 30 July 2019).
- [18] Z. Böcskei, K. Simon, R. Rao, et al., Irbesartan crystal form B, *Acta Crystallogr. Sect. C Cryst. Struct. Commun.* 54 (1998) 808–810.
- [19] Y. Gao, J. Tian, Solubility of irbesartan form B in an aqueous ethanol mixture, *J. Chem. Eng. Data* 53 (2008) 535–537.
- [20] I. Alkorta, I. Rozas, J. Elguero, A computational approach to intermolecular proton transfer in the solid state: assistance by proton acceptor molecules, *J. Chem. Soc. Perkin Trans. 2* (1998) 2671–2676.
- [21] M. Rubčić, K. Užarević, I. Halasz, et al., Desmotropy, polymorphism, and solid-state proton transfer: four solid forms of an aromatic o-hydroxy schiff base, *Chem. Eur. J.* 18 (2012) 5620–5631.
- [22] M. Bauer, R.K. Harris, R.C. Rao, et al., NMR study of desmotropy in Irbesartan, a tetrazole-containing pharmaceutical compound, *J. Chem. Soc. Perkin Trans. 2* (1998) 475–482.
- [23] M.W. Wong, R. Leung-Toung, C. Wentrup, Tautomeric equilibrium and hydrogen shifts of tetrazole in the gas phase and in solution, *J. Am. Chem. Soc.* 115 (1993) 2465–2472.
- [24] V. Jiménez, J.B. Alderete, Complete basis set calculations on the tautomerism and protonation of triazoles and tetrazole, *J. Mol. Struct. THEOCHEM.* 775 (2006) 1–7.
- [25] W.P. Oziminski, The kinetics of water-assisted tautomeric 1,2-proton transfer in azoles: a computational approach, *Struct. Chem.* 27 (2016) 1845–1854.
- [26] G. Chawla, A.K. Bansal, A comparative assessment of solubility advantage from glassy and crystalline forms of a water-insoluble drug, *Eur. J. Pharm. Sci.* 32 (2007) 45–57.
- [27] N. Boutonnet-Fagegaltier, J. Menegotto, A. Lamure, et al., Molecular mobility study of amorphous and crystalline phases of a pharmaceutical product by thermally stimulated current spectrometry, *J. Pharm. Sci.* 91 (2002) 1548–1560.
- [28] A.Y. Lee, D. Erdemir, A.S. Myerson, Crystal polymorphism in chemical process development, *Annu. Rev. Chem. Biomol. Eng.* 2 (2011) 259–280.
- [29] FDA, Scigen Pharmaceuticals, Inc. Issues Voluntary Nationwide Recall of Irbesartan Tablets, USP 75 Mg, 150 Mg, and 300 Mg Due to the Detection of Trace Amounts of NDEA (N-Nitrosodiethylamine) Impurity Found in the Active Pharmaceutical Ingredient (API). <https://www.fda.gov/Safety/Recalls/ucm624593.htm>. (Accessed 30 January 2019).
- [30] S. Veessler, L. Lafferrère, E. García, et al., Phase transitions in supersaturated drug solution, *Org. Process Res. Dev.* 7 (2003) 983–989.
- [31] E. García, C. Hoff, S. Veessler, Dissolution and phase transition of pharmaceutical compounds, *J. Cryst. Growth* 237–239 (2002) 2233–2239.
- [32] E. García, S. Veessler, R. Boistelle, et al., Crystallization and dissolution of pharmaceutical compounds, *J. Cryst. Growth* 198–199 (1999) 1360–1364.
- [33] PDF-4 Organics 2018, ICDD: Newtown Square, PA, 2018, 2018. (Accessed 5 December 2018).
- [34] G. Bartolucci, B. Bruni, M. Di Vaira, et al., 2-Butyl-4-oxo-3-[[2'-(1H-tetrazol-5-yl)biphenyl-4-yl]methyl]-3-aza-1-azoniaspiro[4.4]non-1-ene chloride 1.69-hydrate (irbesartan hydrochloride 1.69-hydrate), *Acta Crystallogr. Sect. E Struct. Reports Online.* 63 (2007) o1529–o1531.
- [35] L. Wang, L.-N. Zhou, Y. Bao, et al., 2-n-Butyl-3-[2'-(1H-tetrazol-5-yl)]

- biphenyl-4-ylmethyl]-1-azonia-3-azaspiro[4.4]non-1-en-4-one bromide sesquihydrate, *Acta Crystallogr. Sect. E Struct. Reports Online*. 63 (2007) o4933–o4933.
- [36] M. Nijhawan, P. Babu, C. Subrahmanyam, Cocrystals of irbesartan with hippuric acid, *Indo Am. J. Pharm. Res.* 5 (2015) 1323–1329.
- [37] C.A. Franca, S.B. Etcheverry, R. Pis Diez, et al., Irbesartan: FTIR and Raman spectra. Density functional study on vibrational and NMR spectra, *J. Raman Spectrosc.* 40 (2009) 1296–1300.
- [38] P. Pangarkar, R.R. Thenge, M.N. Mahajan, et al., Crystal modification of irbesartan in presence of additive, *J. Adv. Pharm. Educ. Res.* 4 (2014) 106–113.
- [39] DRUGBANK, Irbesartan. <https://www.drugbank.ca/drugs/DB01029>, 2017. (Accessed 3 August 2017).
- [40] L. Wang, J. Wang, Y. Bao, et al., Solubility of irbesartan (form A) in different solvents between 278 K and 323 K, *J. Chem. Eng. Data* 52 (2007), 2016–2017.
- [41] L. Yu, Feasibility studies of utilizing disk intrinsic dissolution rate to classify drugs, *Int. J. Pharm.* 270 (2004) 221–227.
- [42] S. Sehić, G. Betz, S. Hadzidedić, et al., Investigation of intrinsic dissolution behavior of different carbamazepine samples, *Int. J. Pharm.* 386 (2010) 77–90.
- [43] S. Byrn, R. Pfeiffer, J. Stowell, *Solid-State Chemistry of Drugs*, 2nd ed., SSCI, Inc., West Lafayette, Indiana, 1999.
- [44] E.H. Lee, A practical guide to pharmaceutical polymorph screening and selection, *Asian J. Pharm. Sci.* 9 (2014) 163–175.
- [45] A.M. Araya-Sibaja, M. Urgellés, F. Vázquez-Castro, et al., The effect of solution environment and the electrostatic factor on the crystallisation of desmotropes of irbesartan, *RSC Adv.* 9 (2019) 5244–5250.